Materials Science Forum
ISSN: 1662-9752, Vol. 925, pp 304-310
doi:10.4028/www.scientific.net/MSF.925.304

Submitted: 2017-08-05
Revised: 2017-12-12
Accepted: 2018-01-11
Online: 2018-06-20

Mechanical Properties and Impact Toughness of Nickel and Aluminum Alloyed High Silicon Ductile Iron

Philipp Weiß[1,a*], Moritz Riebisch[1,b], Andreas Bührig-Polaczek[1,c]

[1]RWTH Aachen University, Foundry-Institute, Intzestraße 5, 52072 Aachen, Germany

[a]p.weiss@gi.rwth-aachen.de, [b]m.riebisch@gi.rwth-aachen.de, [c]sekretariat@gi.rwth-aachen.de

Keywords: High silicon ductile iron, alloy design, mechanical properties, impact toughness

Abstract. High silicon grades of ductile cast iron are known to be highly advantageous in regard to technically relevant properties and economic efficiency. In particular, the outstanding mechanical properties lead to an increasing demand since 2011, the year of incorporation to the EN 1563 standard. However, low impact resistance and spontaneous failure are concerns that limit the application, especially at lower temperatures. Silicon serves as a solid solution strengthener. By the addition of cobalt, aluminum and nickel as additional solid solution strengthener, an improvement in mechanical properties compared to silicon alone could be obtained. Previous studies showed that the addition of 1.5 wt.% Ni to an EN-GJS-500-14 grade with 3.8 wt.% Si resulted in a tensile strength of 650 MPa at 15 % elongation. In the present study, silicon was substituted stepwise by nickel and aluminum, simultaneously aiming at the retention of the mechanical properties of the EN-GJS-500-14 grade. By decreasing the silicon content to 3.3 wt.% Si at 1.1 wt.% Ni and 0.2 wt.% Al, EN-500-14 was obtained. Even though, the presence of pearlite in the matrix was observed, this substitution of silicon led to an increase in Charpy-V-notch toughness by 4 joules at room temperature. For further alloy design of high silicon ductile cast iron for simultaneously substituting silicon and improving the mechanical properties and notch toughness, the restrictions for pearlite formation must be complied.

Introduction

SSF DI (Solid Solution Strengthened Ferritic Ductile Iron) is a modern grade of ductile iron, recently standardized in the European standard DIN EN 1563. Due to the exclusively ferritic matrix, which is stabilized and solid solution strengthened by 3.2 to 4.3 wt.% silicon, the so-called 2nd generation ductile iron grades provide superb mechanical properties in as-casted state [1-5]. At 4.3 wt.% silicon, an ultimate tensile strength (UTS) of 600 MPa at 470 MPa Yield strength (YTS) can be achieved. With a minimum of 10 %, the elongation at fracture is thereby three times higher compared to a 1st generation ductile iron grade of a comparable strength (EN-GJS-600-3). Due to the single-phased ferritic matrix, more uniform properties, such as hardness are obtained throughout the castings when compared to ferritic/perlitic grades, which allow more cost-effective machining [6]. Furthermore, the high amounts of silicon promote the eutectic graphite formation and ensure a stable solidification [7]. The beneficial combination of all mentioned properties leads to an increase in applications during the last decade, e.g. for automotive wheel suspensions, suspension arms, hinge bearings and swing-type housings, hydraulic control blocks as well as rotor hubs and other wind generator components [2, 8-10]. However, some limitations are important to be discussed. Despite the comparatively high elongation at fracture conveys a good ductility, EN-GJS-500-14 exhibits a charpy impact energy of ca. 3 J at RT which is as low as in EN-GJS-500-7. Even though the significance of the charpy impact energy as a restrictive materials property for ductile cast iron is discussed controversially, the low impact energy leads to concerns about spontaneous failure and therefore may restrict the application of SSF DI.

For 1st generation DI grades Hafiz et al. [11] showed that an increased amount of pearlite leads to a decrease in impact energy. The authors varied the pearlite percentage of unalloyed DI from 0 to 95 % via heat treatments, whereas the impact toughness at room temperature was

decreased by up to 76 % at 95 % pearlite. Similar results were obtained by Toktaş et al. [12] for alloyed DI.

The impact energy of fully ferritic DI grades is mainly influenced by the silicon content. Björkegren et al. [13] showed that with an increase of 1 wt.% Si (from 2.74 to 3.74 wt.% Si), the charpy impact energy decreased from 10 to 3 J while the the dutile-brittle transition temperature (DBTT) increased by 85 K. In addition, Gerberich et. al. [14] observed for binary Fe-Si alloys a decrease in cleavage fracture stress and an increase in effective fracture surface energy when the silicon content is decreased. This was attributed to an increase of DBTT by 74 K at 4 at. % Si. In the same study, a decrease in DBTT by 68 K was observed for the addition of 4 at. % Ni in a binary Fe-Ni alloy.

In previous studies, it was proven, that cobalt and nickel can be successfully used as additional solid solution strengthening elements in SSF DI [15-17]. The mechanical properties of EN-GJS-600-10 were reached at 1.5 wt.% Ni and 3.8 wt.% Si.

In the present study, nickel is used as solid solution strengthening element to partially substitute silicon. This approach aims at maintaining the values of UTS, YTS and elongation and additionally increasing the low charpy impact energy of the benchmark grade 500-14. By applying different Ni contents, the influence of Ni, reduction of silicon and restrictions of these features on the above-mentioned properties will be studied. Due to the ferrite-promoting effect and solid solution strengthening, all modified alloys contained 0.2 wt.% aluminum [18].

Experimental Methods

A series of three castings, denoted as alloy 1, alloy 2 and alloy 3, with silicon contents of 3.0, 3.3 and 3.8 wt.% and nickel contents of 0, 1.1 and 1.5 wt.% were produced, as shown in Table 1. The melts were produced from raw materials and prepared using a 50 kg medium frequency induction furnace with a graphite crucible. The nodularisation treatment, inserting a 6.3 wt.% magnesium master alloy (VL 63 M) using a plunger, was conducted after 10 minutes holding time at 1500 °C and deslagging at 1450 °C. Directly after the subsequent inoculation treatment with 0.3 wt.% SMW 605 inoculant, the melt was casted at 1350 °C. For each casting, two sand molds were used containing four Y2 standard blocks (25 mm) each. The sand molds were produced using silica sand and furan resin binder. The chemical composition was determined via spectrometer analysis.

From each alloy, six standardized (DIN 50125 [19]) tensile specimen type A with $d_0 = 8$ mm were extracted from the castings and tested at a cross head speed of 0.6 mm/min. The specimens for microstructural analysis were extracted from the vicinity of the tensile samples. The samples were cold-mounted, ground wet using SiC paper and polished. For the analysis of the pearlite content, the samples were etched using Nital-etching (0.3% HNO_3). The microstructural analysis for optical light micrographs of both unetched and etched was conducted via computational image analysis. For alloy 2 and alloy 3, each 24 Charpy V-notch specimens (5 x 10 x 55 mm, 60° notch, 2 mm deep) were extracted from positions below the tensile samples, machined and tested at -40 °C, -20 °C, 0 °C, 20 °C, 60 °C and 100 °C.

Table 1: Chemical composition of alloys determined using spectrometer analysis.

	Element concentration [wt.%]							
Alloy	C	Si	Ni	Al	Mn	P	S	Mg
1 (3.8Si)	3.16	3.80	0.044	0.006	0.023	0.026	0.009	0.044
2 (3.3Si 1.1Ni 0.2Al)	3.31	3.30	1.09	0.191	0.108	0.018	0.011	0.046
3 (3.0Si 1.5Ni 0.2Al)	3.33	3.03	1.47	0.186	0.105	0.020	0.013	0.044

Results

Microstructure

Figure 1 a) and b) show the etched micrographs of alloy 2 and 3, respectively. The characteristic microstructural features, predominant ferritic matrix with some pearlite and spheritic graphite, can be observed for both alloys. The corresponding results of the image analysis such as nodule count, nodularity and the amount of pearlite are displayed in Table 2 for the three investigated alloys. The standard EN-GJS-500-14 grade (alloy 1) reveals a fully ferritic matrix. For alloy 2 and 3, the amount of pearlite increases with decreasing silicon and increasing nickel content. Compared to the standard grade (alloy 1), both modified alloys show an increased nodule count. An increase in nodularity and a decrease in nodule count was investigated for the increase in nickel content from 1.1 wt.% to 1.5 wt.% and the decrease in silicon content from 3.3 to 3.0 wt.% (alloy 2 vs. alloy 3).

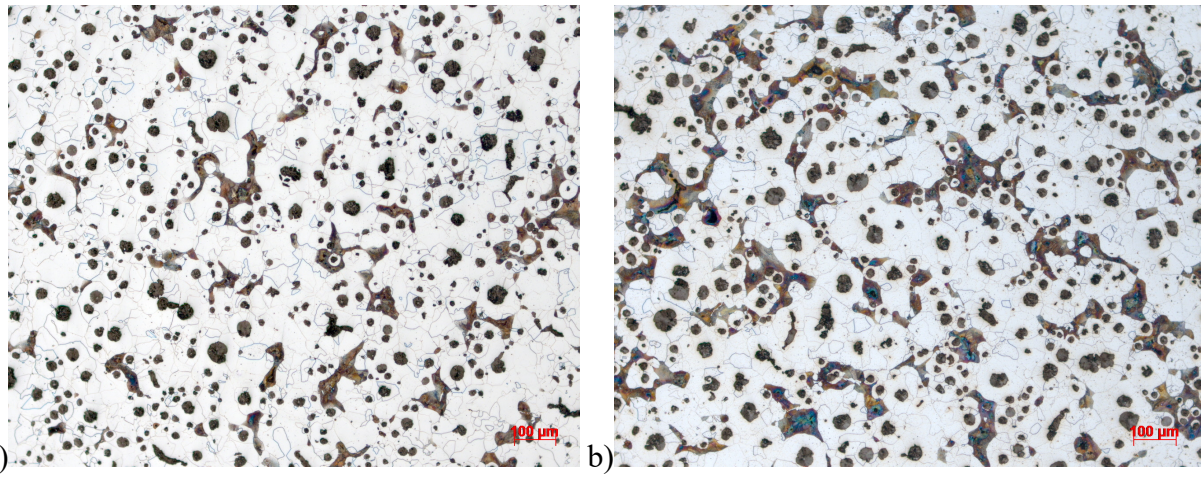

Figure 1: Nital-etched microstructures observed via optical light microscopy of a) alloy 2 with 3.3 wt.% Si, 1.1 wt.% Ni alloy and b) alloy 3 with 3.0 wt.% Si, 1.5 wt.% Ni alloy (alloy 3).

Table 2: Results of the image analysis.

Alloy	Nodularity [%]	Nodule count [1/mm^2]	Pearlite [%]
1 (3.8Si)	83.2	322.7	0
2 (3.3Si 1.1Ni 0.2Al)	72.0	365.8	9.6
3 (3.0Si 1.5Ni 0.2Al)	78.4	350.6	17.2

Mechanical properties

The mechanical properties obtained from the tensile testing are shown in Table 3. All alloys displayed an UTS above 500 MPa and thereby reached or exceeded the targeted strength of 500 MPa. By the decrease of silicon and addition of 1.1 wt.% Ni and 0.2 wt.% Al (alloy 1 vs. alloy 2), a slight decrease in mean UTS of 5.9 MPa and a decrease in mean YTS of 32.1 MPa is obtained. This equals 1 % and 7 %, respectively. The mean elongation is decreased by 4.19 % from 19.93 to 15.73 %. For alloy 3, the further decrease of silicon and increase of nickel to 3.0 and 1.5 wt.%, respectively, resulted in a mean UTS of 585.3 MPa and a mean YTS of 436.7 MPa. In comparison to alloy 1 and 2, this equals an increase in UTS of 4 % and 5 %, respectively, and a difference in YTS of +4 and -3 %, respectively. The decrease of elongation to 12.8 % for alloy 3 is not only considerable but also indicates that this alloy does not reach the targeted elongation of 14 %.

Table 3: Ultimate tensile strength, yield strength and elongation of alloy 1, 2 and 3 obtained from tensile testing.

Alloy	UTS [MPa]	YTS [MPa]	YTS/UTS	Elongation [%]
1 (3.8Si)	563.2 ± 4.99	456.8 ± 4.99	0.81	19.93 ± 1.07
2 (3.3Si 1.1Ni 0.2Al)	557.3 ± 2.31	424.7 ± 2.08	0.76	15.74 ± 0.58
3 (3.0Si 1.5Ni 0.2Al)	585.3 ± 0.57	436.7 ± 1.15	0.75	12.81 ± 0.30

Charpy tests

Figure 2 shows the charpy impact energy as a function of testing temperature for the investigated alloy 2 and alloy 3 as well as reference values from literature [20] for different silicon contents. For temperatures below and at 0 °C, the impact energy of alloy 2 and alloy 3 is 2 J and is therefore identical to the value of the reference with 3.74 wt.% silicon, which shows a similar chemical composition to an EN-GJS-500-14. For increasing temperatures, above 0 °C, an increase in impact energy can be observed; however, no distinct identification of upper-shelf energy and DBTT is possible. At temperatures above 20 °C, alloy 2 shows slightly higher impact energy values for each tested temperature in comparison to alloy 3. For both alloys, the impact energy exceeds the values of the benchmark reference with 3.74 wt.% silicon. Only at very high temperatures (>100 °C) the opposite effect can be observed. All other references, with 3.27 wt.% Si or lower silicon contents, show higher impact energies for all temperatures.

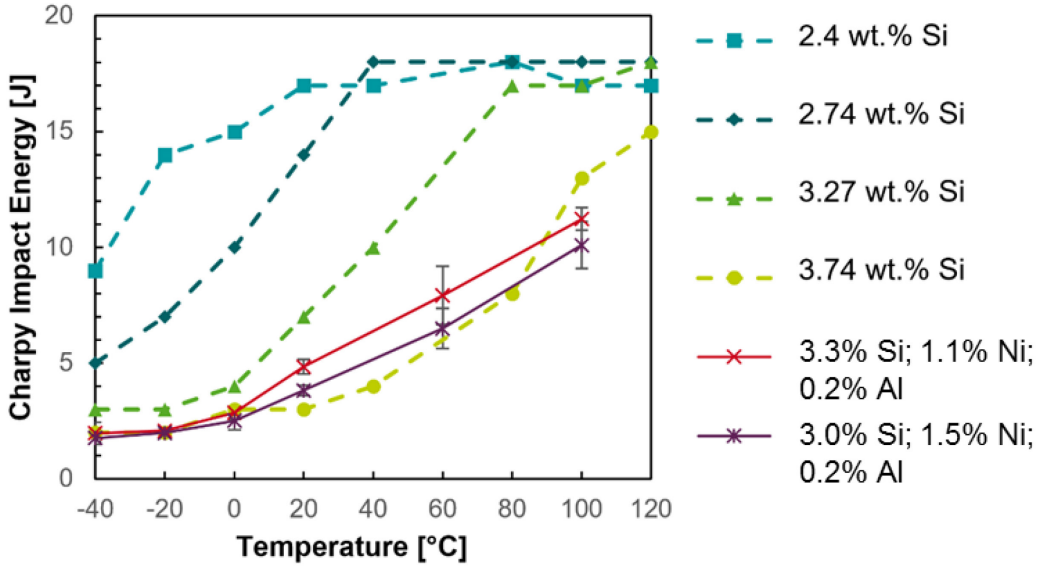

Figure 2: Charpy impact energy at different test temperatures for alloy 2 (3.3 wt.% Si) and alloy 3 (3.0 wt.% Si) in comparison to different alloys without nickel and aluminum from [13].

Discussion

The tensile testing showed that nickel can serve as a substitution element for silicon as similar or higher UTS and YTS were reached for the alloy 2 and alloy 3 with 1.1 and 1.5 wt.% Ni, respectively, in comparison to alloy 1 with 0 wt.% nickel. Even though all alloys showed the targeted UTS of at least 500 MPa, the UTS of alloy 3 with 585.3 ± 0.57 MPa can be considered as slightly too high. Furthermore, for all investigated alloys a strong decrease in elongation with increasing Ni content and decreasing Si content was observed. While the elongation of alloy 2 is still acceptable for EN-GJS-500-14, the elongation of alloy 3 of 12.81 % fails to meet the standard. However, the mechanical properties of alloy 3 with an enhanced UTS and a deteriorated elongation clearly implies the selected chemical composition of alloy 3 is out of scope.

This out-of-scope alloying becomes evident, when the presented findings are elucidated against the background of previous studies. In previous studies, the substitution of Silicon by Ni alloying

on the mechanical properties was investigated for SSF DI with silicon contents between 3.8 to 4.3 wt.%. The (improved) strength values that were obtained by alloying with nickel were compared to similar strength values that were solely achieved by alloying with higher Si contents. This comparison showed that Si- and Ni-containing alloys displayed a favorable combination of strength and elongation in comparison to only Si-containing alloys [15-17]. In contrast to the present study, the elongation-to-strength ratio was diminished less.

The observed pearlite formation can be identified as causal for the decreased elongation-to-strength ratio, which is supported by two findings: Firstly, the DIN EN 1563 standard demands for a solid solution strengthened, fully ferritic EN-GJS-500-14 a higher YTS to UTS ratio than for a pearlite-strengthened EN-GJS-500-7 grade. The decrease in YTS/UTS confirms the strengthening effect of pearlite for alloy 3. Secondly, the previous study was used to calculate the required chemical composition to produce an EN-GJS-500-14 [15-17]. As this calculation only comprised the solid solution strengthening effect of Ni and Si in a fully ferritic matrix and pearlite was observed in the present study, the higher than calculated tensile strength can be attributed to the pearlite.

Therefore, due to the formation of pearlite in the present study, it can be concluded that the contents of nickel as a pearlite-promoting element or of silicon as a ferrite-promoting element were too high or too low, respectively. Despite of this out-of-scope-alloying, this study fundamentally shows that, the principle of the substitution of silicon by other elements (here nickel) is valid. This study therefore displays an expansion of the presented previous study to lower silicon contents and simultaneously the expansion of alloy design and application areas. Additionally, the limit of substitution becomes apparent as alloy 2 already exceeds the standardized maximum pearlite amount of 5 % with 9 % [21]. This limit is expressed by a (not further defined) function of ferrite- and pearlite-promoting elements, here Si and Al against Ni, which needs to be subject of future investigations.

The nodularity, which was decreased by 11.2 and 4.8 % for alloy 2 and alloy 3, respectively, can be evaluated as a further negative influence on the elongation. Lower silicon contents and higher nickel contents are known to promote the nodularity [15]. The lower nodularity of alloy 2 and alloy 3 can therefore only be explained by the addition of aluminum as a ferritizing and solid solution strengthening element. Aluminum is commonly known as a cause for graphite degeneration [22].

Furthermore, this study focusses on the influence of nickel on the Charpy impact energy. An impact energy as low as for the EN-GJS-500-14 (3.74 wt.% Si) was observed for the investigated modified alloys at or below 0 °C. As silicon is known to decrease the impact energy, an increase in the impact energy would have been expected by the decrease of the silicon content. However, the substitution of silicon by nickel displayed no obvious improvement. Due to the reduced ratio of ferrite- and pearlite-promoting elements, pearlite formed in alloy 2 and alloy 3. However, despite of the presence of pearlite, similar impact energy values (and slightly higher values in the range between 20 and 80 °C) in comparison to the fully-ferritic grade 500-14 were gained. A previous quantification [11, 20] showed that 10 % pearlite, which is equal to the pearlite content of alloy 2, led to a decrease in impact energy of 2 to 5 J. When the alloy design is conducted with sub-critical pearlite contents, which can be realized by acceptable silicon and nickel contents, an improvement of the impact energy can be expected. As an alternative to alloy design, a ferritizing heat-treatment may further lead to an improvement of impact energy due to the reduction of pearlite and preservation of solid solution strengthening. Even though the level of impact energy at low temperatures can still be regarded as too low for technical application, further sophisticated optimization has potential for significant improvement.

Conclusions

In the present study, three different solid solution strengthened ductile iron alloys with decreasing silicon content (3.8, 3.3 and 3.0 wt.%) and increasing nickel content (0, 1.1 and 1.5 wt.%) were studied with the focus on nickel as a possible substitutional element for silicon.

The microstructural analysis showed that the required ratio of ferrite-promoting elements, silicon and aluminum, to pearlite-promoting elements, nickel, was undercut. The pearlite content of 9.6 % for alloy 2, containing 3.3 wt.% Si and 1.1 wt.% Ni exceeds the according to DIN-EN-1563 maximum pearlite content of 5 %. The pearlite content of alloy 3 is further increased.

Despite of the unacceptable pearlite content, alloy 2 exhibits the required mechanical properties of an EN-GJS-500-14. Therefore, this study underlines the potential of the approach of reducing the silicon content of fully ferritic SSF DI grades by the substitution of further solid solution strengthening elements. Additionally, a broader alloy spectrum with lower silicon contents is shown to be feasible. The lower limit of silicon substitution by nickel is marked by the chemical composition of alloy 2.

The Charpy impact energies of the investigated nickel-containing alloys, for the application relevant temperatures between -20 and -40 °C, are similar to those of the EN-GJS-500-14. Taking into consideration that the pearlite content has a negative effect on the impact energy, an increase in impact energy by 2 to 5 J in comparison to EN-GJS-500-14 can be expected by avoiding the formation of pearlite. This can either be realized by an alloy design within the allowed limits of the ferritizing-to-pearlitizing-elements ratio or a ferritizing heat-treatment.

Acknowledgements

The authors gratefully acknowledge the valuable suggestions and support of Naemi A. Zumdick, Sebastian F. Fischer, Jessica Frieß, Adalbert J. Kutz and Björn Pustal; the support of Ingo Braun, Dietmar Lembrecht and Dirk Freudenberg, who attended the specimen production, Claus Groten for mechanical testing, Elke Schaberger-Zimmermann for assisting the metallographic analysis; Maria Schaarschmidt for programming the image analysis software, Willie van Balkum at Gieterij Doesburg and Markus Könemann at IEHK RWTH for impact testing and finally the AiF ("Arbeitsgemeinschaft industrieller Forschungsvereinigungen") for the financial support within the AiF-IGF program 18554 N.

References

[1] L. Björkegren, Ferritic ductile iron with higher silicon content, Swedish Foundry Association (941028) (1994).

[2] R. Larker, Solution strengthened ferritic ductile iron ISO 1083/JS/500-10 provides superior consistent properties in hydraulic rotators, 6(4) (2009) 343-351.

[3] A. Alhussein, M. Risbet, A. Bastien, J.-P. Chobaut, D. Balloy, J. Favergeon, Influence of silicon and addition elements on the mechanical behavior of ferritic ductile cast iron, Mater. Sci. Eng. A-Struct 605 (2014) 222-228.

[4] J.R. Davis, Alloying: understanding the basics, ASM international, Materials Park OH, 2001.

[5] C. Labrecque, M. Gagne, Ductile iron: Fifty years of continuous development, Can. Metall. Q. 37(5) (1998) 343-378.

[6] L. Bjorkegren, K. Hamberg, Silicon alloyed ductile iron with excellent ductility and machinability, Hommes et Fonderie(France) 307 (2000) 10-20.

[7] J. Janowak, R. Gundlach, A Modern Approach to Alloying Gray Iron.(Retroactive Coverage), AFS Trans. 90 (1982) 847-863.

[8] J. Goroncy, Neues Gusseisen wiegt Leichtbaudefizite auf, VDI Nachrichten (2004).

[9] K. Herfurth, R. Gorski, K. Beute, M. Hering Gontermann-Peipers, Gopag C 500 F—Gusswerkstoff für den Maschinenbau mit höherer Festigkeit und Bruchdehnung bei sehr homogener Härteverteilung, Giesserei 98(6) (2011) 68.

[10] P. Mikoleizik, G. Geier, SiWind–Werkstoffentwicklung für Offshore-Windenergieanlagen im Multimegawatt-Bereich, Giesserei 9 (2014) 64-69
[11] M. Hafiz, Mechanical properties of SG-iron with different matrix structure, J. Mater. Sci. 36(5) (2001) 1293-1300.
[12] G. Toktaş, M. Tayanc, A. Toktaş, Effect of matrix structure on the impact properties of an alloyed ductile iron, Mater. Charact. 57(4) (2006) 290-299.
[13] L.E. Bjorkegren, K. Hamberg, Silicon Alloyed Ductile Iron with Excellent Ductility and Machinability, Keith Millis Symposium on Ductile Cast Iron (2003).
[14] W. Gerberich, Y. Chen, D. Atteridge, T. Johnson, Plastic flow of Fe-binary alloys—II. Application of the description to the ductile-brittle transition, Acta Metall. 29(6) (1981) 1187-1201.
[15] P. Weiß, J. Brachmann, A. Bührig-Polaczek, S. F. Fischer, Influence of Nickel and Cobalt on the Microstructure of Silicon Solution-strengthened Ductile Iron, Mater. Sci. Technol. (2014).
[16] S.F. Fischer, J. Brachmann, A. Bührig-Polaczek, P. Weiß, Metallurgische Verbesserung von mischkritallverfestigten Gusseisen mit Kugelgrafit: Einfluss von Cobalt und Nickel auf die Mikrostruktur, Giesserei 104(6) (2017) 38-45.
[17] S.F. Fischer, J. Brachmann, A. Bührig-Polaczek, P. Weiß, Metallurgische Verbesserung von mischkritallverfestigten Gusseisen mit Kugelgrafit Teil 2: Einfluss von Cobalt und Nickel auf die mechanischen Eigenschaften, Giesserei 104(7) (2017) 40-51.
[18] F. Neumann, Gusseisen, Expert-Verlag, Renningen-Malmsheim 1999.
[19] DIN Deutsches Institut für Normung e. V., DIN 50125, Prüfung metallischer Werkstofe - Zugproben, Beuth Verlag GmbH, Berlin, Beuth Verlag GmbH, Berlin, 2016.
[20] L. Bjorkegren, K. Hamberg, B. Johannesson, Fachaufsatze-Mechanische Eigenschaften und Bearbeitbarkeit von mit Silicium verfestigten ferritischen Gusseisen mit Kugelgraphit-Einfluss von Silicium-Hartestreuungen-Vergleich mit GJS-500-7, Giesserei Praxis (1) (1999) 11-17.
[21] DIN Deutsches Institut für Normung e. V., DIN EN 1563:2012-03, Gießereiwesen – Gusseisen mit Kugelgraphit, Beuth Verlag GmbH, Berlin, 2012.
[22] T. Thielemann, Zur Wirkung von Spurenelementen im Gusseisen mit Kugelgraphit, Giessereitechnik 16(1) (1970) 16-24.